Seasonality of the transpiration fraction and its controls across typical ecosystems within the Heihe River Basin

Yaqin Tong[1], Pei Wang[1]*, Xiao-Yan Li[1]*, Lixin Wang[2], Xiuchen Wu[1], Fangzhong Shi[1], Yan Bai[1], Engui Li[1], Jiaqi Wang[1], Yang Wang[1]

[1] State Key Laboratory of Earth Surface Processes and Resource Ecology, Faculty of Geographical Science, Beijing Normal University, Beijing, 100875, China.

[2] Department of Earth Sciences, Indiana University-Purdue University Indianapolis, Indianapolis, IN 46202, USA

Corresponding author: first and last name: Pei Wang (peiwang@bnu.edu.cn)， Tel: 0086-10-58800148, Fax: 0086-10-58800148； Xiao-Yan Li, xyli@bnu.edu.cn, Tel: 0086-10-58802716, Fax: 0086-10-58802716

Accepted Article

Key Points:

- Transpiration fraction were evaluated with *in-situ* measurements of isotope approach, sap flow, and uWUE method across five ecosystems
- Cropland with the highest transpiration fraction, followed by alpine meadow, desert riparian forest, shrub, and alpine swamp meadow
- Leaf area index exerts a first-order control of transpiration fraction, other environment factors further explain divergence

This is the author's manuscript of the article published in final edited form as:

Tong, Y., Wang, P., Li, X.-Y., Wang, L., Wu, X., Shi, F., … Wang, Y. (2019). Seasonality of the transpiration fraction and its controls across typical ecosystems within the Heihe River Basin. Journal of Geophysical Research: Atmospheres, 0(ja). https://doi.org/10.1029/2018JD029680

Abstract

Understanding the seasonality of the transpiration fraction (T/ET) of total terrestrial evapotranspiration (ET) is vital for coupling ecological and hydrological systems and quantifying the heterogeneity among various ecosystems. In this study, a two-source model was used to estimate T/ET in five ecosystems over the Heihe River Basin (HRB). *In-situ* measurements of daily energy flux, sap flow, and surface soil temperature were compared with model outputs for 2014 and 2015. Agreement between model predictions and observations demonstrates good performance in capturing the ecosystem seasonality of T/ET. In addition, sensitivity analysis indicated that the model is insensitive to errors in measured input variables and parameters. T/ET among the five sites showed only slight inter-annual fluctuations while exhibited significant seasonality. All the ecosystems presented a single-peak trend, reaching the maximum value in July and fluctuating day to day. During the growing season, average T/ET was the highest for the cropland ecosystem (0.80 ± 0.13), followed by the alpine meadow ecosystem (0.79 ± 0.12), the desert riparian forest *Populus euphratica* (0.67 ± 0.07), the *Tamarix ramosissima Ledeb* desert riparian shrub ecosystem (0.67 ± 0.06), and the alpine swamp meadow (0.55 ± 0.23). Leaf area index exerted a first-order control on T/ET and showed divergence among the five ecosystems because of different vegetation dynamics and environmental conditions (e.g., water availability or vapor pressure deficits). This study quantified transpiration fraction across diverse ecosystems within the same water basin and emphasized the biotic controls on the seasonality of the transpiration fraction.

Keywords: Transpiration fraction, Two source model, Arid Inland Heihe River Basin, Seasonality, Sensitivity analysis, Typical ecosystems

Plain Language Summary

The management of water resources in Heihe River Basin (HRB) requires accurate predictions of water yield. At present, the response of the ecosystem of this river basin to regional climate change is faced with many uncertainties. Transpiration fraction（T/ET), is an important index to measure different vegetation feedback on climate change. Quantify T/ET and analysis the differences across typical ecosystems within HRB is of great scientific and practical significance for the sustainability development in the future.

Accepted Article

© 2019 American Geophysical Union. All rights reserved.

1 Introduction

Evapotranspiration (ET), including soil/canopy evaporation (E) and plant transpiration (T), is the main component of terrestrial ecosystem energy and water balance (Aouissi et al., 2016; Good et al., 2015; Zhou et al., 2016a; Sulman et al., 2016). The transpiration fraction (T/ET), as an indicator of evapotranspiration partition, plays an important role in qualifying vegetation-climate feedbacks and improving future hydrological prediction (Jasechko et al., 2013; Maxwell and Condon, 2016; Wang et al., 2014; Zhu et al., 2016). Globally, transpiration accounts for 64 ± 13% of evapotranspiration by global isotope-budget (Good et al., 2015), and 62 ± 6% of evapotranspiration by CMIP5 (Lian et al., 2018). Transpiration represents the largest loss of water from ecosystems (Berkelhammer et al., 2016; Sun et al., 2014a) and the quantification of T/ET still faces many uncertainties. Understanding the seasonality of T/ET can reveals details of the processes that underlie ecosystem hydrological budgets and their feedback to the water cycle (Li et al., 2013a; Kool et al., 2014b; Velpuri & Senay, 2017; Wen et al., 2016a; Zhao et al., 2016a). The T/ET can vary between 20% and 95% across ecosystems (Berkelhammer et al., 2016). T/ET studies across a wide spectrum of scales and ecosystems have become a hotspot in ecohydrology and related disciplines (Hu et al., 2017; Velpuri & Senay, 2017; Zhou et al., 2016a) to improve the prediction of ecosystem responses to climate change.

Many methods can be used to estimate T/ET, including measuring devices such as lysimeters, sap flow sensors (Davis et al., 2012; Uddin et al., 2011; Bai et al., 2017), isotopic approaches (Sun et al., 2014b; Wen et al., 2016a; Wang et al., 2010; Zhang et al., 2010), and models (Abera et al., 2017; Diarra et al., 2017; Singh et al., 2017; Zhou et al., 2016b). Among many methods, the modeling approach has the advantage of applying over a wide range of temporal and spatial scales (Shuttleworth et al., 2000). There were many models with different complexity can be used for modeling evapotranspiration and its components. The one source models (e.g., Penman and Penman-Monteith resistance models) are the simplest one but only estimate total ET flux. The multi-source models account for the vertical heterogeneity of surface conditions and/or spatial heterogeneity by dividing the surface into multiple patches (Zhang et al., 2016, Wang et al., 2018). However, they suffer from larger uncertainties because they need extensive variable/parameter inputs (Were et al., 2008). A two-source model is a useful tool to estimate ET and its components (Shuttleworth & Wallace, 2010; Norman & Becker, 1995; Wang & Yamanaka, 2014). Although a two-source model does not consider the interception loss term, it still provides reasonable estimates of

Accepted Article

© 2019 American Geophysical Union. All rights reserved.

T/ET across various ecosystems (Norman et al., 2003; Anderson et al., 2004; Li et al., 2008; Song et al., 2016a). As reviewed by Kool et al., (2014), despite measurement variability of ~30%, the past studies showed over 90% agreement for ET = E + T without considering other possible sources (e.g., interception). Previous investigations indicated that forest ecosystems have larger interception ratio, but for grassland ecosystems the contribution of interception loss to total ET is much smaller (Cui et al., 2017). In arid areas, where precipitation is rare, canopy-intercepted precipitation contribution to total ET is small and can be negligible (Wang et al., 2018).

The Heihe River is the second largest inland river in China and is located in the arid and semiarid area of northwestern China. It is characterized by a complex geographical environment, a unique water resource system, and a coexistence of frozen circles and arid areas that is not available in other arid regions of the world (Zhao & Cheng, 2008). Quantifying vegetation feedbacks are important in regional climate models to investigate the basin-scale water recycling and improve integrated water resource management. So far, vegetation feedback is largely uncertain in climate models in terms of future predictions (Wang et al., 2018). Evapotranspiration represents the greatest loss of water balance in this area, and transpiration is the main component of terrestrial water flux, which is sensitive to changes in vegetation types and dynamics (Berkelhammer et al., 2016; Zhou et al., 2016a). Moreover, improving irrigation efficiency may require partitioning ET to improve irrigation water management. Several previous studies have been conducted in this area to estimate T/ET. Zhao et al. (2016) used an *in-situ* observation method to estimate that transpiration accounts for about 64% of water loss in the Heihe River Basin (HRB) desert shrub ecosystem. Wen et al. (2016) used the isotopic technique combined with the eddy covariance (EC) technique to partition ET in a maize ecosystem. However, previous studies have been conducted at different time scales and/or locations with different approaches, and no comprehensive comparison and assessment among various ecosystems have been performed. So far, few studies have addressed the partitioning of ET along environment gradients (altitude, precipitation and temperature) in the HRB across typical ecosystems from upper, middle, and downstream reaches and accessed the controls of water flux using the same protocol. Zhou et al. (2018) used uWUE method, both determined from eddy covariance ET and GEP to partition ET in three typical ecosystems from upper to lower reaches within the HRB, this method requires periods when T/ET=1 and such requirement is rarely met in water-limited ecosystems. The present study used ET measured by the EC system and

© 2019 American Geophysical Union. All rights reserved.

Accepted Article

transpiration measured with TDP (thermal dissipation probes) combined with a two-source model to estimate ET and T/ET. The objectives were: (1) to estimate the seasonality of T/ET across typical ecosystems in the HRB over a two-year period; (2) to explain the convergence and divergence of T/ET across different ecosystems in the HRB; and (3) to clarify the controls for seasonal variations of T/ET and to establish a quantitative relationship between T/ET and vegetation cover indices (e.g., leaf area index, (LAI) across different ecosystems.

2 Materials and Methods

2.1 **Study sites**

The HRB, located between 97.1° and 102.0°E and between 37.7° and 42.7°N, contains the second largest inland river in China, originating from the Qilian Mountains glacier snow belt (**Figure 1**). The total area of HRB is 14.3 million km^2 which integrates alpine glaciers, grassland, plain oases, and the Gobi desert from upper to lower reaches(Cheng et al., 2014a; Zhao et al., 2014). In the upper reaches in the Qilian Mountains, at an altitude between 1674 and 5564 m, the climate is cold and arid. With characteristics of wet and cold (average annual temperature of 0.54°C) and an average annual precipitation of 300–600 mm, the vegetation spatial distribution is more obvious in the vertical zone, which is the runoff-generated area in the basin. The main runoff area is located at an altitude above 3600 m and consists of glaciers, sparse alpine vegetation, and alpine meadows. The middle reaches, at an altitude between 1352 and 1700 m, have a temperate continental arid climate with an annual average precipitation of 90–160 mm and an annual evaporation of 2000–2500 mm. The vegetation type is natural and artificial oases, which are the areas with the greatest intensity of human activity. The lower reaches have an altitude less than 1352 m and are more arid, with rare precipitation and strong evapotranspiration. The average annual temperature is 8.7°C, the average annual rainfall is 36.6 mm, and the vegetation is mainly desert and riparian forest (Si et al., 2013). There are series of hydrometeorological observatory in the upstream, midstream and downstream of the HRB (Li et al., 2013b; Liu et al., 2011), covering the main vegetation types of the HRB. In the present study, the alpine meadow and alpine swamp meadow ecosystems in the upper reaches, the cropland ecosystem in the middle reaches, and the *Tamarix ramosissima Ledeb* and *Populus euphratica* ecosystems in the lower reaches were selected for investigation. All sites have continuous observation data from EC systems and automatic weather stations (AWS) from January 2014 to December 2015. Table 1 lists detailed descriptions of each ecosystem, and Figure 2 shows the meteorological conditions of each ecosystem in 2014 and 2015.

© 2019 American Geophysical Union. All rights reserved.

Accepted Article

2.2 Data

The observation data were obtained from a hydrometeorological observation network dataset provided by Heihe Watershed Allied Telemetry Experimental Research (HiWATER) (*http://hiwater.westgis.ac.cn/*), which includes EC systems and AWS. The data collection has been described in details in earlier studies (Liu et al., 2011; Xu et al., 2013). The EC systems were mounted on towers ranging from 3.5 to 22 m above the various canopy heights (Table 1). Post-processing calculations were performed using EdiRe (Li et al., 2013b; Liu et al., 2011), and the results were gap-filled using a set of general algorithms (Reichstein et al., 2005). After gap-filling, daily energy budget closure was used to evaluate the EC data, which was determined by the linear regression statistics between (LE+H) and (R_n-G) (Liu et al., 2011b). The energy balance closure for the daily-mean datasets ranged from 74% to 96% (Figure 3), which indicated that energy balance closure issue in our sites was not big. Meteorological data including air temperature (T_a, °C), humidity (RH, %), wind speed (u, m s^{-1}), air pressure (P, Pa), surface soil temperature at a depth Z_{soil} (T_s,°C), volumetric soil water content (θ, m^3 m^{-3}), downward solar radiation (S_d, W m^{-2})， were used for model input. All the energy fluxes including net radiation (R_n, W m^{-2}), sensible and latent heat flux (H and LE, W m^{-2}) and soil heat flux (G, W m^{-2}), as well as transpiration data for *P. euphratica* measured with sap flow (Li et al., 2017; Qiao et al., 2015) at the Hunhelin site (obtained from http://www.heihedata.org/) were used to test model performance. The GLASS leaf area index (LAI) products (http://glassproduct.bnu.edu.cn/) from Beijing Normal University (Xiao et al., 2016), available every 8 days and interpolated into a daily time interval, were used to represent vegetation dynamics in this study. Vegetation heights of riparian forest in the lower reaches were acquired by a field quadrat survey, and vegetation heights of alpine meadow in the upper reaches were obtained by reference to a research dataset of ecohydrology transects in the HRB in 2013 (Feng et al., 2014). The heights of maize in cropland attained from Wen et al. (2016).

2.3 Model description

A two-layer source model was used to estimate T/ET. The main equations of the model are illustrated in supplementary materials (Text S1). This model was chosen for the following reasons: First, this model, using the energy balance between the soil surface and the vegetation canopy and taking into account the energy interaction between them, achieved good performance in partitioning ET in the humid grasslands of Japan (Wang and Yamanaka, 2014; Wang et al., 2015), the cropland ecosystem of the HRB (Wang et al., 2016), and arid

© 2019 American Geophysical Union. All rights reserved.

Accepted Article

and semiarid grassland in Inner Mongolia in China (Wang et al., 2018). Second, the model uses the Newton-Raphson iteration scheme to solve the governing equations for the canopy and the ground surface separately without the need for radiometric temperature. Third, the model considers stomatal control of transpiration, including its dependence on soil moisture, and solar radiation is explicitly included. The model was localized to fit the characteristics of each ecosystem. Table S1 summarizes the parameters used for each site in this study. More details about the model can be found in Wang and Yamanaka (2014).

2.4 Model performance assessment and sensitivity analysis

As summarized by Willmott (1981), the root mean square error (RMSE) and I index, as well as R^2 (R is the correlation coefficient), were used to validate and test the model. The I index is defined as:

$$\mathrm{I} = 1 - \frac{\sum_{j=1}^{n}\left(p_{j-o_j}\right)2}{\sum_{j=0}^{n}\left(|p_{j-\sigma}|+|o_{j-\sigma}|\right)^2} \quad , \tag{1}$$

where the p_j are predicted values, the o_j are observed values, σ is the mean value of the o_j, the subscript j denotes measurement number, and n is the total number of measurements. The value of I is unity for perfect agreement and zero for no agreement between observations and predictions.

To evaluate possible errors in the specified model parameters or measurement variables, a sensitivity analysis of the input variables is necessary. The method proposed by (Qiu et al., 1998) and (Wang & Yamanaka, 2014) was selected. To quantify the influence of the driving variables and parameters on evapotranspiration and its components in the model, a sensitivity coefficient (S_i) can be defined as:

$$s_i = \frac{\partial O}{\partial P_i}\frac{P_i}{O}, \tag{2}$$

where P_i is the i-th driving parameter or variable that can affect the output (O, such as LE or T/ET). The partial derivative $\frac{\partial O}{\partial P_i}$ can be computed by the following equation:

$$\frac{\partial O}{\partial P_i} = \frac{O_p^* - O_p}{P_i^* - P_i}, \tag{3}$$

where O_p^* is the O predicted by the model with a provisionally assumed value of P_i (i.e., P_i^*) and O_p is the predicted O with P_i assigned in the model or measured. s_i= 0.1 means that an increase of 1% in P_i causes an increase of 0.1% in the output result O. The negative sensitivity coefficient indicates that a reduction in the output result O is caused by an increase

© 2019 American Geophysical Union. All rights reserved.

in P_i, and vice versa.

3 Results

3.1 Model validation and performance

Compared to the measured values, all the energy fluxes were reasonably simulated (Table 2). At the apline (swamp) meadow, and cropland ecosystems, which are located in the upper and middle reaches of the HRB, good agreement can be seen for all the energy fluxes, with the RMSE ranging from 4.12 to 38 W m^{-2} and the I index ranging from 0.63 to 0.96. At the *T. ramosissima* and *P. euphratica* ecosystems, which are located in the lower reaches, the model showed good performance for LE, R_n, and G, with RMSE ranging from 6.61 to 39.75 W m^{-2}, but slightly higher RMSE (57.00 and 69.98 W m^{-2}) for H simulations. Although the simulation of H is less than ideal, the day-to-day variation of LE was well simulated and nonsystematic among the five typical ecosystems during the study period (Figure 4). The validity of our modeling can be reflected not only by energy fluxes but also by temperature information such as ground surface temperature (T_G). The measured T_G is in good agreement with the predicted T_G in the five typical ecosystems (Figure 5). The measured daily vegetation transpiration by sap flow at the Hunhelin site was used for comparison with modeling results. The predicted T values were in good agreement with the measured values with R^2 equaling to 0.75 and 0.80 in 2014 and 2015, respectively (Figure 6b and 6c). To further validate the modeled ET partitioning results, we collected all the available T/ET data from previous studies conducted in the cropland ecosystem using isotope method along with the lysimeter/eddy covariance measurements (Wen et al., 2016) and uWUE (underlying water use efficiency) approach (Zhou et al., 2018). Figure 7a illustrates the comparison of hourly–mean T/ET values simulated by our model with the ones estimated by isotope approach and by uWUE method in the early afternoon. In addition, the daily-mean T/ET values simulated by our model and by lysimeter/eddy covariance and uWUE methods are shown in Figure 7b. Generally, the T/ET values estimated using our model were more steady than the other two methods at both hourly and daily time scales. The simulated T/ET values were larger than the ones estimated by uWUE method, and the simulated T/ET trend was more consistent with the values estimated by isotope approach and the lysimeter/eddy covariance method. Consequently, the T/ET estimated by the two source model should be reasonable within the HRB.

Accepted Article

© 2019 American Geophysical Union. All rights reserved.

3.2 Sensitivity analysis

Table 3 summarizes the sensitivity analysis results for measured variables in different ecosystem types. RH was the most sensitive variable for LE in the upper and middle reaches. A 5% error in RH could cause errors of 3.7%, 2.4%, and 6.25% at the apline meadow, apline swamp meadow and cropland ecosystems, respectively. In the riparian forest in the lower reaches, T_a is the most sensitive variable for LE; a 5% error in T_a could cause an error close to 3.5% in LE. As for T/ET, LAI was the most sensitive variable in all ecosystems; a 5% error in LAI would cause errors of 2.2%, 4.15%, 2.75%, 3.95%, and 2.85% in T/ET at the apline meadow, apline swamp meadow, cropland, *T. ramosissima*, and *P. euphratica* ecosystems, respectively. The values of *Si* for T/ET were small in all the five studied ecosystems, indicating that modeled results are insensitive to errors of measured variables.

3.3 Spatiotemporal dynamics of T/ET

T/ET showed significant seasonality among the five ecosystems, with smaller interannual fluctuations. All ecosystems presented a single-peak trend, reaching the maximum value in July and fluctuating day to day (Figure 8). For the whole year, the mean annual T/ET was highest in cropland (0.53 ± 0.26), followed by *P. euphratica* (0.52 ± 0.17), apline meadow (0.51 ± 0.26), *T. ramosissima* (0.50 ± 0.20), and apline swamp meadow (0.31 ± 0.28). For the growing season (May–September) only, mean T/ET value was also highest in cropland (0.80 ± 0.13), followed by apline meadow (0.79 ± 0.12), *P. euphratica* (0.67 ± 0.07), *T. ramosissima* (0.67 ± 0.06) and apline swamp meadow (0.55 ± 0.28). The higher T/ET values during growing season meant transpiration played an important role in water vapor fluxes in these ecosystems. About 60% of the field is covered with plastic films in the cropland ecosystem，bare soil evaporation is significantly reduced. While for *T. ramosissima* and *P. euphratica* ecosystems, there were very few precipitation events during the study period, surface is dry, but T could remain constant because plants can draw deeper water. The swamp meadow ecosystem was located at higher elevations, surface had plentiful water, T/ET was lowest during the growing season.

3.4 Controlling factors of transpiration fraction

Figure 9 shows the relationship between LAI and T/ET in the five ecosystems. The strong relationships ($R^2 > 0.69$) indicate that the seasonality of T/ET was mainly controlled by vegetation dynamics characterized by LAI variations. The relationship between LAI and

© 2019 American Geophysical Union. All rights reserved.

Accepted Article

T/ET was stronger for the alpine (swamp) meadow and cropland ecosystems with higher R^2s (> 0.91) than for the downstream riparian ecosystems (0.69–0.73). This indicates that in upper and middle reaches LAI can explain >90% of the variations in ecosystem T/ET, whereas in the extremely arid riparian ecosystem, other environmental factors (e.g., water availability, vapor pressure deficit) or biotic factors (e.g., rooting depth) also affect T/ET. To further analyze the impact of other environmental factors on T/ET, spearman rank correlation analysis (Jerrold, 1972) was conducted. Based on the results in Table 4, all the variables were strongly correlated with T/ET illustrating the complex interactions among vegetation, atmosphere and soil.

4 Discussion

4.1 Seasonality of T/ET in different ecosystems in the Heihe River Basin

Understanding the seasonality of T/ET across ecosystems is vital to discern the vegetation feedback to the climate system and improve predictions of future hydrological changes in the HRB. Table 5 summarizes results from previous studies on evapotranspiration partition and compares these results with those obtained in this study. The growing season average and annual mean of T/ET in the alpine swamp meadow were 0.31 and 0.55, respectively, which are similar to the previously reported values (0.40 and 0.59) in the Haibei alpine swamp meadow (Hu et al., 2009). Our modeled mean annual T/ET value in this study is the same with the results from Zhou et al. (2018) but discrepancy exists in the growing season. Our modeled result is higher than what is reported in Zhou et al. (2018) during the growing season. Cropland ecosystem in middle reaches had the largest T/ET value, which is consistent with Zhou et al. (2014; 2018), who found that cropland had higher T/ET than other vegetation types. The mean values of T/ET of the Daman site in the early afternoon (13:00–15:00) are 0.86 ± 0.06 using the isotope method (Wen et al., 2016) and 0.88 ± 0.06 using the two-source variation data assimilation (TVDA) method during the growing season (Xu et al., 2016). These values are higher than the daily mean values of 0.80 ± 0.13 found in this study. Wei et al. (2017) stated that most isotope-based studies report higher transpiration fraction than non-isotope-based measurements. Zhao et al. (2016) used sap flow measurements in the middle reaches of the HRB and found that T/ET of the *Calligonum* shrub ecosystem was about 0.66 during the growing season (May–September) from 2008 to 2010, which is similar to the result obtained here (0.67 ± 0.06) for the *T. ramosissima* shrub ecosystem.

© 2019 American Geophysical Union. All rights reserved.

Comparisons indicate that T/ET varied among the different ecosystems in the HRB and the modeling results are comparable with the available results within the HRB using other observation methods. At the same time, the results also indicate that it is difficult to compare results among different ecosystems when observations are obtained using different methods because of possible mismatches at the temporal and spatial scales or different uncertainties associated with different techniques.

4.2 Convergence and divergence of T/ET among different ecosystems

As shown in Figure S2, transpiration is directly related to vegetation activity, and therefore, it is not surprising that LAI strongly controls T/ET (Hu et al., 2009; Wang et al., 2014; Wang & Yamanaka, 2014; Wei et al., 2017). Our results showed that LAI could explain more than 80% of the day-to-day variations of T/ET across meadow and cropland ecosystems (Figure 9), but the percentage dropped to about 70% for downstream *P. euphratica* and *T. ramosissima* shrub ecosystems. However, it is still not clear to what extent T/ET ratios controlled by vegetation and what additional factors could further explain T/ET variations in different ecosystems. Wang et al. (2014) developed a plant growth stage function to achieve a further explanation of global variation in T/ET under the same LAI condition. Under the same LAI condition (e.g., LAI =0.5), the T/ET values were 0.61, 0.52, 0.62, 0.68, and 0.69 at the A'rou, Dashalong, Daman, Sidaoqiao, and Hunhelin sites, respectively. As shown in Figure S2, we found largest variations of monthly LAI in A'rou but relatively smaller variations of T/ET, followed by Daman, while for downstream ecosystems, such as Huhelin and Sidaoqiao, there are smaller changes of monthly LAI, but results in larger changes of T/ET. Dashalong site is in the middle situation. Therefore, apart from LAI, soil moisture and atmospheric condition also contributed to these variations. Generalized linear model (GLM) analyses (Pei et al., 2017; Wu et al., 2018) were used to investigate the relative contribution of all the variables to T/ET changes in different ecosystems. We found that LAI played an important role in controlling T/ET variations in all ecosystems, followed by soil moisture in the upper and middle reaches. While in the riparian ecosystems, the contribution of atmospheric conditions (VPD) is higher than soil moisture (Table 6). The results obtained here indicate that T/ET has a convergent evolution that is controlled by internal ecosystem characteristics (e.g., LAI dynamics) and T/ET also shows divergences among ecosystems because of different environmental conditions.

Accepted Article

© 2019 American Geophysical Union. All rights reserved.

4.3 Uncertainty analysis

In this study, T/ET was simulated using a two-layer source model. The modeling results agree well with the available observations. However, some uncertainties remained. On one hand, uncertainties may arise from the model input variables. To explore this possibility, sensitivity analysis was carried out to determine the effect of the main input variable variations on T/ET. The result showed that T/ET was more sensitive to LAI and soil water content than to the other variables. LAI was the most sensitive factor, and therefore the uncertainties in the modeling output may be related to uncertainty in the LAI data set. Different LAI products exhibited discrepancies. However, the LAI products used here had been extensively validated by field measurements in the study area, their effects on T/ET should be small. On the other hand, soil water content also affected the modeling results. By combining previous studies on water uptake by vegetation roots (Amos & Walters, 2006; Himmelbauer et al., 2010; Yue et al., 2015) and imposing constraints on temperature and energy flux, it was determined that 10-cm soil moisture was suitable for representing water availability in the alpine, swamp meadow, and cropland ecosystems, whereas 100–120 cm soil moisture was best in the riparian ecosystem. Use of soil moisture from different layers could result in estimated T/ET errors of less than 6% over the whole year (**Figure 10**), and larger differences in T/ET were mainly apparent in the non-growing season.

Besides, evaporation of rainfall intercepted by the vegetation was not considered in the present model, this may have resulted in overestimation of T/ET in alpine (swamp) meadow ecosystems, because precipitation amount is small in other ecosystems in the HRB (annual precipitation is about 150 mm in the cropland and is about 30 mm in the riparian ecosystems). To qualify the uncertainties caused by interception in the upper alpine meadow ecosystem and alpine swamp meadow, ET partition results (T/ET) were compared for the rain/entire dataset (n=258/604) and sunny days only (n= 346), respectively. Statistical results indicate that there was no significant difference ($p>0.05$) for T/ET between the datasets for rain (entire) and sunny days. The errors caused by intercepted rainfall account for < 2% (1%) for T/ET in alpine meadow ecosystem (alpine swamp meadow). Therefore, although there are possible errors in the model simulations, the ET partition results are quite robust and reasonable. Consequently, the potential error caused overestimation T/ET by interception is not big issue in our study.

5. Conclusions

This study used a two-layer source model to estimate T/ET across typical ecosystems

© 2019 American Geophysical Union. All rights reserved.

Accepted Article

over the HRB. The good agreement obtained between simulation and observations of energy flux, ground soil temperature, transpiration measured by sap flow, and estimated T/ET by previous studies indicates that the model performed well. Sensitivity analysis indicated that the model is not sensitive to uncertainties in the measured input variables. In the Heihe River Basin, except alpine swamp meadow, the mean annual T/ET values among alpine meadow, cropland, *T. ramosissima* shrub and *P. euphratica* ecosystems were similar, but the seasonality of T/ET was significant. The results obtained here indicate that LAI is a first-order controlling factor for T/ET and that other factors (e.g., soil water dynamics and vapor pressure deficit) result in divergence of T/ET among ecosystems. The results of this study highlight that T/ET exhibits a convergent evolution that controlled by internal ecosystem characteristics (e.g., LAI dynamics) and expresses various divergences among ecosystems because of different environmental conditions.

Accepted Article

© 2019 American Geophysical Union. All rights reserved.

Acknowledgments

The study was financially supported by the National Natural Science Foundation of China (91425301 and 41671019) and by the State Key Laboratory of Earth Surface Processes and Resource Ecology. LW acknowledges summer support from the Division of Earth Sciences of National Science Foundation (NSF EAR-1562055 and 1554894) and the President's International Research Awards from Indiana University. We thank all the scientists, engineers, and students who participated in the HiWATER field campaigns. The observed dataset can be downloaded at http://heihedata.org/hiwater. We thank Dr. Sha Zhou from the Department of Earth and Environmental Engineering Columbia University, who provided T/ET estimations using the stable isotope, lysimeter/eddy covariance and uWUE data at the cropland ecosystem.

Accepted Article

© 2019 American Geophysical Union. All rights reserved.

References:

Abera, W., Formetta, G., Borga, M. & Rigon, R. (2017). Estimating the water budget components and their variability in a pre-alpine basin with JGrass–NewAGE. *Advances in Water Resources*, 104: 37–54. doi:10.1016/j.advwatres.2017.03.010.

Amos, B. & Walters, D.T. (2006). Maize root biomass and net Rhizodeposited Carbon. S*oil Science Society of America Journal*, 70(5): 1489. doi:10.2136/sssaj2005.0216.

Aouissi, J., Benabdallah, S., Lili Chabaâne, Z. & Cudennec, C., (2016). Evaluation of potential evapotranspiration assessment methods for hydrological modelling with SWAT–Application in data-scarce rural Tunisia. *Agricultural Water Management*, 174: 39–51.

Bai Y, X. Li., S. Liu., P. Wang. (2017). Modelling diurnal and seasonal hysteresis phenomena of canopy conductance in an oasis forest ecosystem. *Agricultural and Forest Meteorology*, 246: 98–110.

Berkelhammer, M., Noone, D. C., Wong, T. E., Burns, S. P., Knowles, J. F., Kaushik, A., Blanken, P. D. & Williams, M. (2016). Convergent approaches to determine an ecosystem's transpiration fraction. *Global Biogeochemical Cycles*, 30(6): 933–951. doi: 10.1002/2016GB005392.

Cheng, G., Li, X., Zhao, W., Xu, Z., Feng, Q., Xiao, S., Xiao, H. (2014). Integrated study of the water-ecosystem-economy in the Heihe River Basin. Natl. Sci. Rev. 1,413–428.

Cui, Y.K., Zhao, P., Yan, B., Xie, H., Yu, P., Wan, W., Fan, W.J., & Hong,Y. (2017). Developing the remote sensing-gash analytical model for estimating vegetation rainfall interception at very high resolution: a case study in the heihe river basin. *Remote Sensing*, *9*(7), 661.

Diarra, A., Jarlan, L., Er-Raki, S., Page, M. L., Aouade, G., Tavernier, A., Boulet, G., Ezzahar, J., Merlin, O. & Khabba, S. (2017). Performance of the two-source energy budget (TSEB) model for the monitoring of evapotranspiration over irrigated annual crops in North Africa. *Agricultural Water Management*, 193: 71–88.

Good, S.P., Noone, D. & Bowen, G. (2015). Hydrologic connectivity constrains partitioning of global terrestrial water fluxes. *Science*, 349(6244): 175.

Himmelbauer, M., Loiskandl, W. & Rousseva, S. (2010). Spatial root distribution and water uptake of maize grown on field with subsoil compaction. *Journal of Hydrology and Hydromechanics*, 58(3). doi: 10.2478/v10098-010-0015–z.

Hu, Z., Yu, G., Zhou, Y., Sun, X., Li, Y., Shi, P., Wang, Y., Song, X., Zheng, Z., Zhang, L. & Li, S. (2009). Partitioning of evapotranspiration and its controls in four grassland ecosystems: Application of a two-source model. *Agricultural and Forest Meteorology*, 149(9): 1410–1420. doi: 10.1016/j.agrformet.2009.03.014.

Hu, Z., Wu, G., Zhang, L., Li, S., Zhu, X., Zheng, H., Zhang, L., Sun, X. & Yu, G. (2017). Modeling and Partitioning of Regional Evapotranspiration Using a Satellite–Driven Water-Carbon Coupling Model. *Remote Sensing*, 9(1).

Huang, X., Hao, Y., Wang, Y., Wang, Y., Cui, X., Mo, X. & Zhou, X. (2010). Partitioning of evapotranspiration and its relation to carbon dioxide fluxes in Inner Mongolia steppe. *Journal of Arid Environments*, 74(12): 1616–1623.

Jasechko, S., Sharp, Z. D., Gibson, J. J., Birks, S.J., Yi, Y., & Fawcett, P.J., (2013). Terrestrial water fluxes dominated by transpiration. *Nature*, 496(7445):347.

Jerrold, H. Zar., (1972). Significance Testing of the Spearman Rank Correlation Coefficient. *Journal of the American Statistical Association*, 67:339, 578-580.

Kelliher, F.M., Leuning, R. & Schulze, E.D. (1993). Evaporation and canopy characteristics of coniferous forests and grasslands. *Oecologia*, 95(2): 153–163.

Koetz, B., Baret, F., Poilvé, H. & Hill, J. (2005). Use of coupled canopy structure dynamic and radiative transfer models to estimate biophysical canopy characteristics. *Remote Sensing of Environment*, 95(1): 115–124.

Kool, D., Agam, N., Lazarovitch, N., Heitman, J. L., Sauer, T. J. & Ben-Gal, A. (2014). A review of approaches for evapotranspiration partitioning. *Agricultural and Forest Meteorology*, 184: 56–70.

Li, X., Cheng, G., Liu, S., Xiao, Q., Ma, M., Jin, R., Che, T., Liu, Q., Wang, W. & Qi, Y. (2013). Heihe watershed allied telemetry experimental research (HiWATER): Scientific objectives and experimental design. *Bulletin of the American Meteorological Society*, 94(8): 1145–1160.

Li, X., Liu, S., Xiao, Q., Ma, M., Jin, R., Tao, C., Wang, W., Hu, X., Xu, Z. & Wen, J. (2017). A multiscale dataset for understanding complex eco–hydrological processes in a heterogeneous oasis system. *Scientific Data*, 4: 170083.

Lian, X., Piao, S.L., Chris, H., Li, Y., Zeng, Z.Z., Wang, X.H., Ciais, P., McVicar, T.R., Peng, S.S., Ottlé, C.,Yang, H., Yang, Y.T., Zhang, Y.Q., & Wang, T. (2018). Partitioning global land evapotranspiration using CMIP5 models constrained by observations. *Nature Climate Change*, 8(7): 640-646.

Liu, B., Guan, H., Li, S., Zhao, W. & Yang, Y. (2017). Groundwater facilitated water-use efficiency along a gradient of groundwater depth in arid northwestern China. *Agricultural and Forest Meteorology*, 233: 235–

© 2019 American Geophysical Union. All rights reserved.

241.
Liu, S., Xu, Z., Wang, W., Jia, Z., Zhu, M., Bai, J., & Wang, J. (2011). A comparison of eddy-covariance and large aperture scintillometer measurements with respect to the energy balance closure problem. *Hydrology Earth System Science* 15, 1291–1306.
Liu, S., Xu, Z., Zhu, Z., Jia, Z., &Zhu, M. (2013). Measurements of evapotranspirationfrom eddy-covariance systems and large aperture scintillometers in the HaiRiver Basin, China. *Journal of Hydrology* 487, 24–38.
Maxwell, R.M. & Condon, L.E. (2016). Connections between groundwater flow and transpiration partitioning. *Science*, 353(6297): 377.
Willmott CJ. (1981). On the validation of models. *Physical Geography* 2: 184–194.
Norman JM, Becker F. (1995). Terminology in thermal infrared remote sensing of natural surfaces. *Agricultural and Forest Meteorology* 77: 153–166
Nagler, P.L., Glenn, E.P., Thompson, T.L., & Huete, A. (2004). Leaf area index and normalized difference vegetation index as predictors of canopy characteristics and light reception by riparian species on the Lower Colorado River. *Agricultural and Forest Meteorology*, 125(1): 1–17.
Pei, T., Wu, X.C., Li, X.Y., Zhang, Y., Shi,F.Z., Ma,Y.J., Wang,P.,& Zhang,C. (2017). Seasonal divergence in the sensitivity of evapotranspiration to climate and vegetation growth in the Yellow River Basin, China. *Journal of Geophysical Research*: *Biogeosciences*, 122(1): 103-118.
Qiao, C., Sun, R., Xu, Z., Zhang, L., Liu, L., Hao, L. & Jiang, G. (2015). A Study of Shelterbelt transpiration and cropland evapotranspiration in an irrigated area in themiddle reaches of the Heihe River in Northwestern China. IEEE *Geoscience and Remote Sensing Letters*, 12(2): 369–373.
Qiu, G.Y., Yano, T. & Momii, K. (1998). An improved methodology to measure evaporation from bare soil based on comparison of surface temperature with a dry soil surface. *Journal of Hydrology*, 210(1–4): 93–105.
Reichstein, M., Falge, E., Baldocchi, D., Papale, D., Aubinet, M., Berbigier, P., Bernhofer, C., Buchmann, N., Gilmanov, T. & Granier, A . (2005). On the separation of net ecosystem exchange into assimilation and ecosystem respiration: review and improved algorithm. *Global Change Biology*, 11(9): 1424–1439.
Song, L.S., Liu, S.M., Kustas, W. P., Zhou, J., Xu, Z.W., Xia, T., & Li, M.S. (2016). Application of remote sensing-based two-source energy balance model for mapping field surface fluxes with composite and component surface temperatures. *Agricultural and Forest Meteorology*, *230-231*, 8-19.
Su, P., Li, S., Zhou, Z., Rui, S. & Xie, T. (2016). Partitioning evapotranspiration of desert plants under different water regimes in the inland Heihe River Basin, Northwestern China. *Arid Land Research & Management*, 30(2): 1–15. doi:org/10.1080/15324982.2015.1061616.
Singh, S., Boote, K.J., Angadi, S.V. & Grover, K.K. (2017). Estimating water balance, evapotranspiration and water use efficiency of spring safflower using the CROPGRO model. *Agricultural Water Management*, 185: 137–144.
Sun, S., Meng, P., Zhang, J., Wan, X., Zheng, N. & He, C. (2014). Partitioning oak woodland evapotranspiration in the rocky mountainous area of North China was disturbed by foreign vapor, as estimated based on non-steady-state ^{18}O isotopic composition. *Agricultural and Forest Meteorology*, 184: 36–47. doi:10.1016/j.agrformet.2013.08.006.
Sulman, B. N., D. T. Roman., T. M. Scanlon., L. Wang, & K. A. Novick. (2016). Comparing methods for partitioning a decade of carbon dioxide and water vapor fluxes in a temperate forest, *Agricultural and Forest Meteorology*, 226-227, 229-245. doi:http://dx.doi.org/10.1016/j.agrformet.2016.06.002.
Shuttleworth W J., & Wallace J S. (2010). Evaporation from sparse crops–an energy combination theory. *Quarterly Journal of the Royal Meteorological Society*, 111(469):839–855.
Velpuri, N.M. & Senay, G.B. (2017). Partitioning Evapotranspiration into Green and Blue Water Sources in the Conterminous United States. *Scientific Reports*, 7(1): 6191.
Wang, D. & Wang, L. (2017). Dynamics of evapotranspiration partitioning for apple trees of different ages in a semiarid region of northwest China. *Agricultural Water Management*, 191: 1–15.
Wang, L., S. P. Good., & K. K. Caylor. (2014). Global synthesis of vegetation control on evapotranspiration partitioning, *Geophysical Research Letters*, 41, 6753–6757. doi:10.1002/2014GL061439.
Wang, L., Caylor, K. K., Villegas, J. C., Barron-Gafford, G. A., Breshears, D. D., & Huxman, T. E. (2010). Partitioning evapotranspiration across gradients of woody plant cover: assessment of a stable isotope technique, *Geophysical Research Letters*, *37*, L09401. doi:10.1029/2010GL043228.
Wang, L., Wei, X., Bishop, K., Reeves, A. D., Ursino, N., and Winkler, R. (2018).Vegetation changes and water cycle in a changing environment, *Hydrology Earth System Science*, 22, 1731-1734. https://doi.org/10.5194/hess-22-1731-2018.
Wang, P., Li, X.Y., Huang, Y., Liu, S., Xu, Z., Wu, X. Ma, Y. (2016). Numerical modeling the isotopic composition of evapotranspiration in an arid artificial oasis cropland ecosystem with high–frequency water vapor isotope measurement. *Agricultural and Forest Meteorology*, 230–231: 79–88.

© 2019 American Geophysical Union. All rights reserved.

doi:10.1016/j.agrformet.2015.12.063.
Wang, P. & Yamanaka, T., (2014). Application of a two-source model for partitioning evapotranspiration and assessing its controls in temperate grasslands in central Japan. *Ecohydrology*, 7(2): 345–353. doi:10.1002/eco.1352.
Wang, P., Li, X.Y., Wang, L.X., Wu, X.C., Hu, X., Fan,Y., Tong, Y.Q.(2018). Divergent evapotranspiration partition dynamics between shrubs and grasses in a shrub-encroached steppe ecosystem. *New Phytologist*, 219(4), 1325-1337. http://doi:10.1111/nph.15237.
Wang-Erlandsson, L., van der Ent, R.J., Gordon, L.J., Savenije, H.H.G. (2014). Contrasting roles of interception and transpiration in the hydrological cycle – Part 1: Temporal characteristics over land. *Earth System Dynamics*, 5(2): 441–469. doi:10.5194/esd–5–441–2014.
Wei, Z., Yoshimura, K., Wang, L., Miralles, D., Jasechko, S. & Lee, X. (2017). Revisiting the contribution of transpiration to global terrestrial evapotranspiration. *Geophysical Research Letters*, 44: 2792–2801.
Wen, X., Yang, B., Sun, X., & Lee, X. (2016). Evapotranspiration partitioning through in-situ oxygen isotope measurements in an oasis cropland. *Agricultural and Forest Meteorology*, 230–231: 89-96. doi:10.1016/j.agrformet.2015.12.003.
Were, A., Villagarcía, L., Domingo, F., Moro, M.J. & Dolman, A.J. (2008). Aggregating spatial heterogeneity in a bush vegetation patch in semi-arid SE Spain: A multi-layer model versus a single-layer model. *Journal of Hydrology*, 349(1-2): 156-167.
Wu, Y., Du, T., Ding, R., Tong, L., Li, S., & Wang, L. (2017).Multiple methods to partition evapotranspiration in a maize field. *Journal of Hydrometeorology*, 18(1): 139–149.
Wu, X., Liu, H., Li, X., Ciais, P., Babst, F., Guo, W., et al. (2018). Differentiating drought legacy effects on vegetation growth over the temperate northern hemisphere. *Global Change Biology*, 24(1), 504–516. https://doi.org/10.1111/gcb.13920
Xu, T., Bateni, S. M., Margulis, S. A., Song, L., Liu, S., & Xu, Z. (2016). Partitioning evapotranspiration into soil evaporation and canopy transpiration via a two-source variational data assimilation system. *Journal of Hydrometeorology*, *17*(9), 2353–2370.
Xu, Z., Liu, S., Li, X., Shi, S., Wang, J., Zhu, Z., Xu, T., Wang, W., & Ma, M. (2013). Intercomparison of surface energy flux measurement systems used during the HiWATER- MUSOEXE. *Journal of Geophysical Research Atmospheres*, 118(23): 13140–13157.
Zhang, K., Kimball, J. S., & Running, S. W. (2016). A review of remote sensing based actual evapotranspiration estimation: a review of remote sensing evapotranspiration. *Wires Water*, *3*(6), 834-853.
Zhang, S., Wen, X., Wang, J., Yu, G., & Sun, X. (2010). The use of stable isotopes to partition evapotranspiration fluxes into evaporation and transpiration. *Acta Ecologica Sinica*, 30(4): 201–209.
Zhao, W., Liu, B., Chang, X., Yang, Q., Yang, Y., Liu, Z., Cleverly, J., & Eamus, D. (2016). Evapotranspiration partitioning, stomatal conductance, and components of the water balance: A special case of a desert ecosystem in China. *Journal of Hydrology*, 538: 374–386. doi: 10.1016/j.jhydrol.2016.04.042.
Zhao, L., L. Wang., X. Liu., H. Xiao., Y. Ruan., & M. Zhou. (2014). The patterns and implications of diurnal variations in the d-excess of plant water, shallow soil water and air moisture. *Hydrology and Earth System Sciences*, *18*(10), 4129-4151. doi:10.5194/hess-18-4129-2014.
Zhou, S., Yu, B., Zhang, Y., Huang, Y., & Wang, G. (2016). Partitioning evapotranspiration based on the concept of underlying water use efficiency. *Water Resources Research*, 52(2): 1160–1175. doi:10.1002/2015WR017766.
Zhou, S., Yu, B., Zhang, Y., Huang, Y., & Wang, G. (2018). Water use efficiency and evapotranspiration partitioning for three typical ecosystems in the Heihe River Basin, northwestern China. *Agricultural and Forest Meteorology*, 253–254: 261–273. doi: 10.1016/j.agrformet.2018.02.002.
Zhu, G., Zhang, K., Li, X., Liu, S., Ding, Z., Ma, J., Huang, C., Han, T., & He, J. (2016). Evaluating the complementary relationship for estimating evapotranspiration using the multi-site data across north China. *Agricultural and Forest Meteorology*, 230-231: 33–44. doi: 10.1016/j.agrformet.2016.06.006.
Qi, F., Yonghong, S., Hong, H., Yong, Z., & Haining, G. (2014). Dataset of investigation of eco-hydrology transect in Heihe river basin. *Heihe Plan Science Data Center*. doi:10.3972/heihe.041.2014.db.
Wang, Q., Yang, W., Huang, J., Xu, K., & Wang, P. (2017). Shrub encroachment effect on the evapotranspiration and its component—A numerical simulation study of a shrub encroachment grassland in Nei Mongol, China. *Chinese Journal of Plant Ecology*, 41(03), 348–358. doi: 10.17521/cjpe.2016.0236.
Wang, Z., Zhang, H., Wang, Y., & He, C. (2016). Diurnal variations of grassland evapotranspiration over different periods in the Pailugou basin in the upper reach of the Heihe River, Northwest China. *Chinese Journal of Applied Ecology*, 27(11): 3495–3504. doi: 10.13287 / j.1001–9332.201611.012.
Yang, Y., Chen, R. S., Song, Y. X., Liu, J. F., Han, C. T., & Liu, Z. W. (2013). Measurement and estimation of grassland evapotranspiration in a mountainous region at the upper reach of Heihe River basin, China. *Chinese Journal of Applied Ecology*, 24(04): 1055–1062.
Yue, G., Zhao, L., Wang, Z., Zou, D., Zhang, L., & Qiao, Y. (2015). Relationship between alpine meadow root

© 2019 American Geophysical Union. All rights reserved.

distribution and active layer temperature variation in permafrost areas. *Journal of Glaciology and Geocryology*, 37(5):1381–1387.

Zhao, W., & Cheng, G. (2008). Frontier issues and experimental observational ecohydrology. *Advances in Earth Science*, 23(07): 671–674.

Accepted Article

© 2019 American Geophysical Union. All rights reserved.

Table 1 *Main characteristics of the typical ecosystems in the Heihe River Basin*

Site	Longitude	Latitude	Altitude (m)	Dominant vegetation type	EC height(m)	Watershed positions
A'rou	100.46°E	38.05°N	3044	Alpine meadow	3.5	Upstream
Dashalong	98.94°E	38.84°N	3739	Alpine swamp meadow	4.5	
Daman	100.37°E	38.86°N	1556	Cropland	4.5	Midstream
Hunhelin	101.13°E	41.99°N	874	*P. euphratica*	22	Downstream
Sidaoqiao	101.14°E	42.00°N	873	*T. ramosissima*	8	

***Note**: EC height means the heights eddy covariance systems were mounted above the canopy heights.*

Accepted Article

© 2019 American Geophysical Union. All rights reserved.

Table 2

Model performance statistics with daily mean data in the five typical ecosystems

Site	Index	Energy flux			
		LE	R_n	H	G
A'rou	R^2	0.91	0.85	0.29	0.42
	I	0.96	0.95	0.75	0.63
	RMSE (W m^{-2})	16.02	23.08	20.86	8.23
	n	711	730	730	730
Dashalong	R^2	0.8	0.71	0.45	0.73
	I	0.95	0.91	0.86	0.98
	RMSE (W m^{-2})	20.18	31.7	24.52	9.86
	n	724	719	720	730
Daman	R^2	0.84	0.93	0.34	0.7
	I	0.94	0.96	0.83	0.98
	RMSE (W m^{-2})	23.67	26	38	11.35
	n	669	730	730	730
Hunhelin	R^2	0.84	0.96	0.29	0.86
	I	0.95	0.88	0.47	0.67
	RMSE (W m^{-2})	27.4	34.55	69.98	8.81
	n	673	730	730	730
Sidaoqiao	R^2	0.78	0.92	0.4	0.82
	I	0.89	0.89	0.65	0.89
	RMSE (W m^{-2})	38.61	32.1	57	6.61
	n	716	730	699	730

Note: LE is latent heat flux, Rn is net radiation, H is sensible heat flux, G is ground heat flux, RMSE (W m^{-2}) is root mean square error, R^2 is the coefficient of determination and n is the number of data points.

Accepted

© 2019 American Geophysical Union. All rights reserved.

Table 3

Mean and standard deviation (SD) of the sensitivity coefficients of LE and T/ET to the measured variables

Site	Variables	Mean ±SD			
		Ta	RH	LAI	θ
A'rou	LE	0.52 ± 0.38	-0.74 ± 0.32	0.16 ± 0.09	0.22 ± 0.06
	T/ET	0.19 ± 0.27	0.00 ± 0.22	0.44 ± 0.28	0.34 ± 0.28
Dashalong	LE	0.05 ± 0.04	-0.48 ± 0.22	0.13 ± 0.43	0.13 ± 0.13
	T/ET	0.02 ± 0.21	0.20 ± 0.22	0.83 ± 0.48	0.29 ± 0.35
Daman	LE	0.63 ± 0.35	-1.25 ± 0.70	0.29 ± 0.26	0.39 ± 0.18
	T/ET	0.04 ± 0.16	0.08 ± 0.18	0.55 ± 0.34	0.43 ± 0.32
Hunhelin	LE	0.72 ± 0.40	-0.37 ± 0.27	0.26 ± 0.16	0.19 ± 0.22
	T/ET	0.08 ± 0.06	0.00 ± 0.11	0.79 ± 0.42	0.36 ± 0.45
Sidaoqiao	LE	0.65 ± 0.31	-0.34 ± 0.32	0.23 ± 0.10	0.11 ± 0.14
	T/ET	0.02 ± 0.03	0.09 ± 0.12	0.57 ± 0.22	0.15 ± 0.20

Note: LE means latent heat flux, Ta means air temperature, RH means relative humidity, LAI means Leaf area index, θ means soil water content.

Accepted Article

© 2019 American Geophysical Union. All rights reserved.

Table 4

Spearman correlation coefficients between T/ET and several variables

Site	LAI[a]	VPD[b]	R_n[c]	θ[d]	Ta[e]
A'rou	0.94**	0.63**	0.72**	0.76**	0.88**
Dashalong	0.95**	0.57**	0.79**	0.76**	0.84**
Daman	0.98**	0.69**	0.80**	0.92**	0.92**
Sidaoqiao	0.92**	0.87**	0.82**	0.42**	0.88**
Hunhelin	0.88**	0.89**	0.70**	0.56**	0.91**

Note: ** means significant correlation at the 0.01 significance level, LAI means Leaf area index, VPD means vapor pressure deficit, R_n means net radiation, θ means soil water content and Ta means air temperature.

Accepted Article

© 2019 American Geophysical Union. All rights reserved.

Table 5

Summary of transpiration fraction (T/ET) and RMSE for observed and predicted energy fluxes in the Heihe River Basin

Literature	Method	Vegetation type	Time Scale	RMSD (W m^{-2})				T/ET	
				lE	R_n	H	G	Growing season	All year
Xu et al., 2016	TVDA model	Cropland	Hourly	116	10.1	27.3	30.2	0.88 ± 0.06	N/A
Wang et al, 2016	Iso-SPAC model	Cropland	Hourly	45.9	45.16	51.4	21.37	0.88 ± 0.13	N/A
Wen et al., 2016	Situ oxygen isotope	Cropland	Hourly	N/A	N/A	N/A	N/A	0.86 ± 0.06	N/A
Su et al., 2016	Lysimeters	*T. ramosissima*	Daily	N/A	N/A	N/A	N/A	0.37-0.50	N/A
Zhao et al, 2016	Sap flow measurement	*Calligonum L.*	Daily	N/A	N/A	N/A	N/A	0.64	N/A
Zhou et al, 2018	uWUE	Alpine meadow	Daily	N/A	N/A	N/A	N/A	0.55	0.51
		Cropland		N/A	N/A	N/A	N/A	0.63	0.52
		P. euphratica		N/A	N/A	N/A	N/A	0.55	0.53
This study	Two source model	Alpine meadow	Daily	16.02	23.8	20.86	8.23	0.79 ± 0.12	0.51± 0.26
		Alpine swamp meadow		20.18	31.7	24.52	9.86	0.55 ± 0.23	0.31 ± 0.28
		Cropland		23.67	26	38	11.35	0.80 ± 0.13	0.53 ± 0.26
		P. euphratica		27.4	34.55	69.98	8.81	0.67 ± 0.07	0.52 ± 0.17
		T. ramosissima		38.61	32.1	57	9.86	0.67 ± 0.06	0.50 ± 0.20

Accepted Article

© 2019 American Geophysical Union. All rights reserved.

Table 6

The relative contributions of environment factors to variations of transpiration fraction (T/ET) in five ecosystems

Site	[a]LAI (%)	[b]VPD (%)	[c]R_n (%)	[d]θ (%)	[e]T_a (%)
A'rou	70	3.86	1.7	18	0.13
Dashalong	90	1.6	0.77	2.43	0.03
Daman	87	2.6	1.12	4.1	0.66
Sidaoqiao	56	10	0.08	0.65	4.3
Hunhelin	68	14	0.04	10	0.79

Note. [a] Leaf area index, [b] vapor pressure deficit, [c] net radiation, [d] soil water content, [e] air temperature.

Accepted Article

© 2019 American Geophysical Union. All rights reserved.

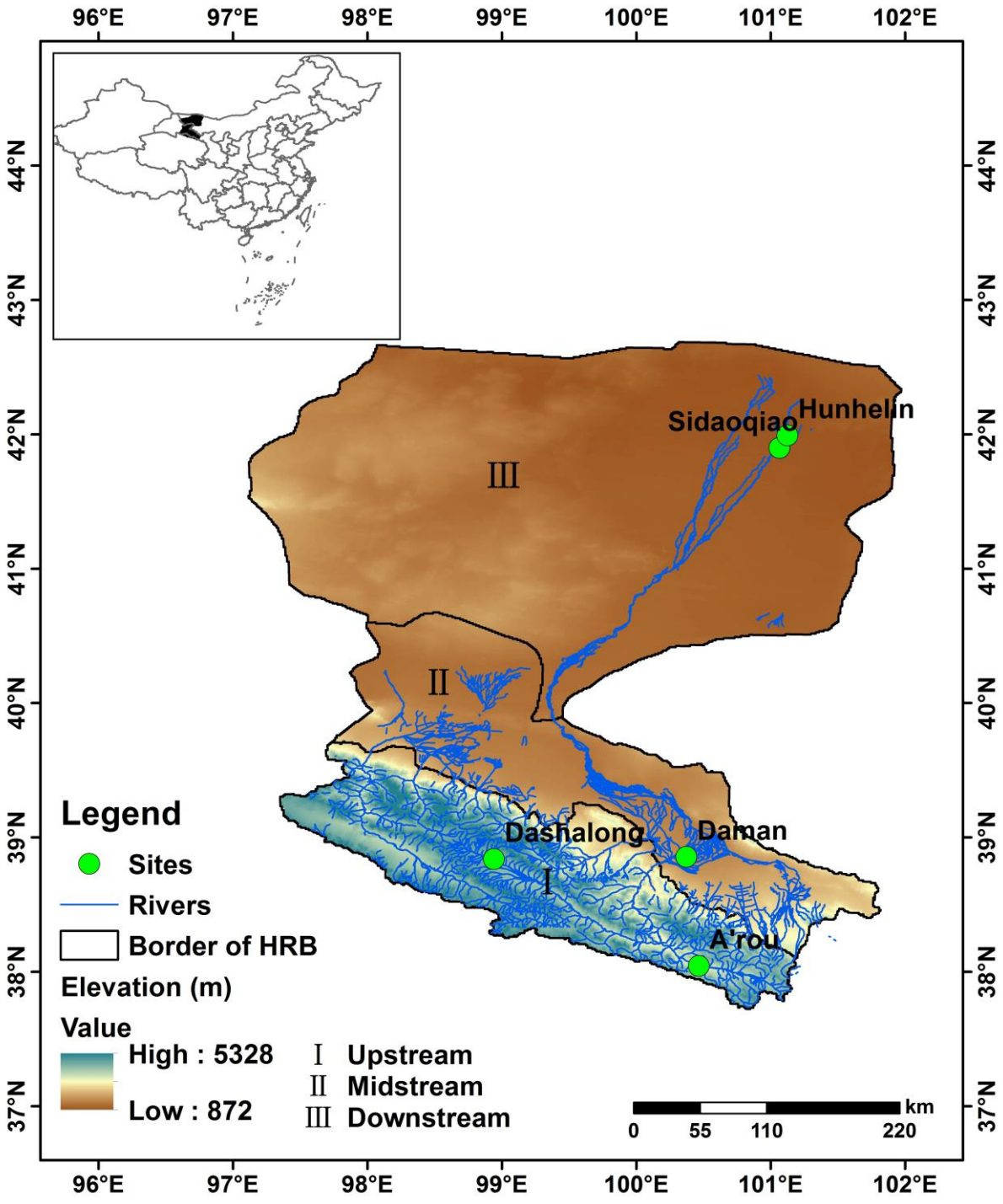

Figure 1. Topography and location of the study sites within the Heihe River Basin.

© 2019 American Geophysical Union. All rights reserved.

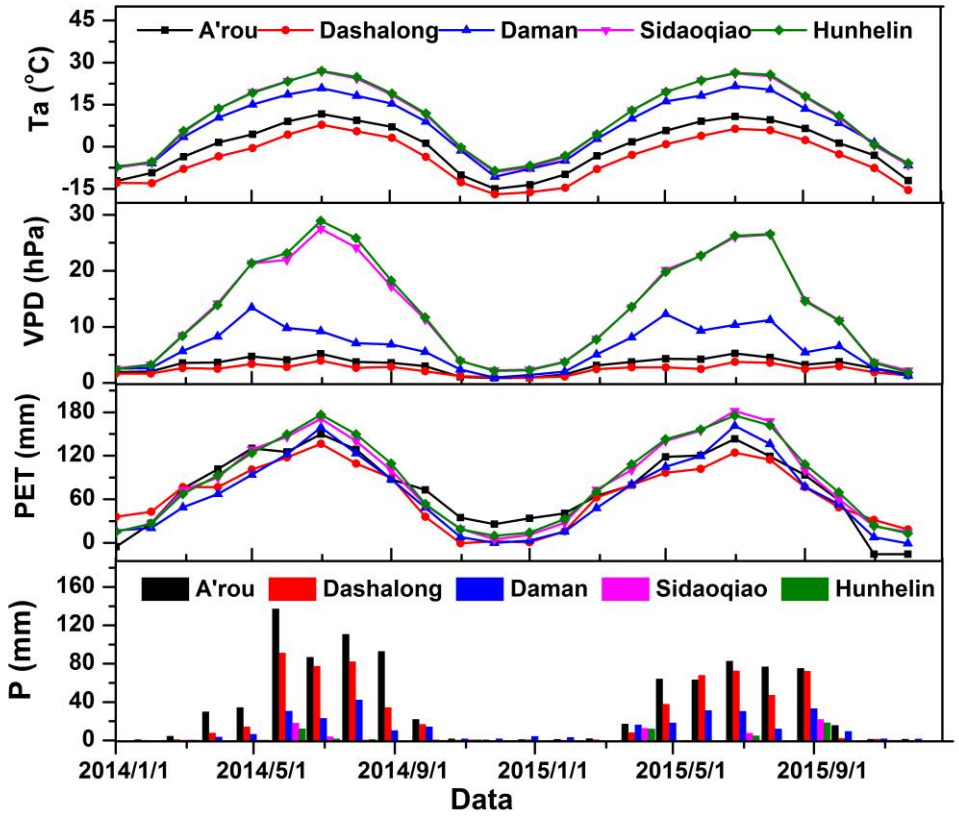

Figure 2. Meteorological factors in typical ecosystems from 2014 to 2015, mean monthly air temperature (T_a, °C), vapor pressure deficit (VPD, hPa), potential evapotranspiration (PET, calculated with FAO Penman Monteith equation) and precipitation (P, mm) for A'rou (alpine meadow ecosystem), Dashalong (alpine swamp meadow ecosystem), Daman (cropland ecosystem), Sidaoqiao (*T .ramosissima* ecosystem), and Hunelin (*P. euphratica* ecosystem) sites.

Accepted

© 2019 American Geophysical Union. All rights reserved.

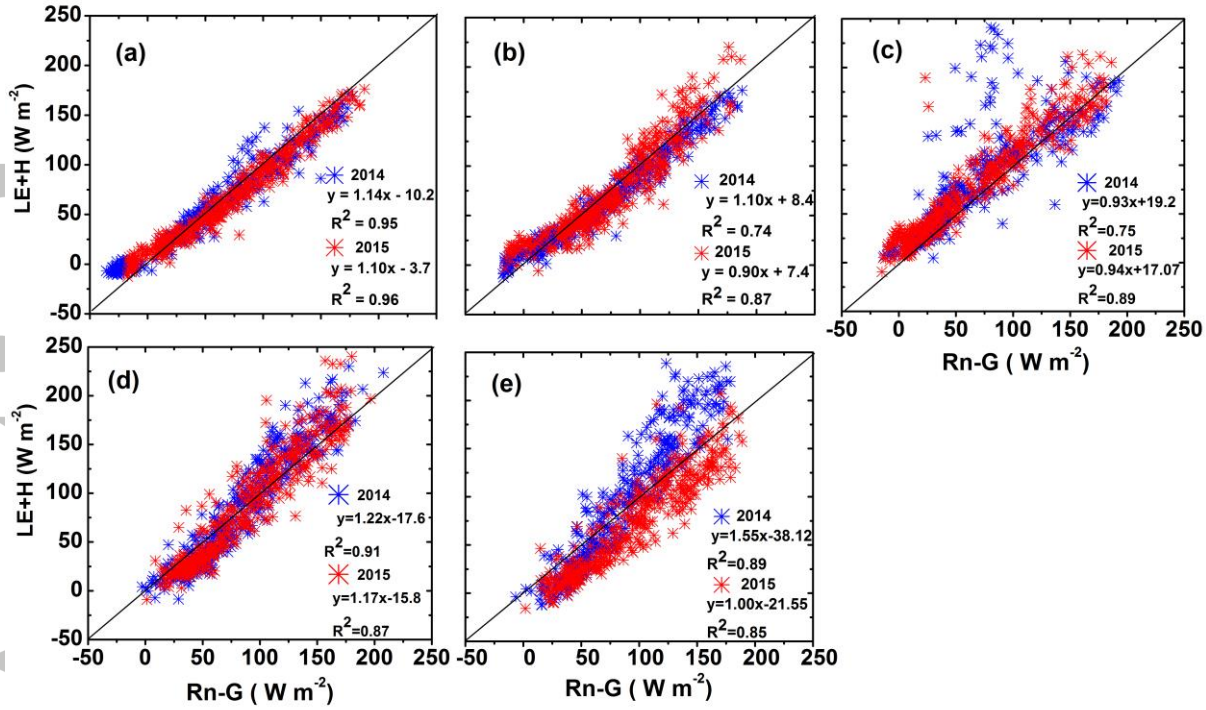

Figure 3. Regression relationship between sums (LE+H) of latent heat flu (LE) and sensible heat flux (H) and available energy (R_n-G) expressed by abstraction between net radiation (R_n) and ground heat flux (G) based on daily eddy covariance data at (a) alpine meadow, (b) alpine swamp meadow, (c) cropland, (d) *T. ramosissima*, (e) *P. euphratica* ecosystem in 2014 and 2015.

Accepted

© 2019 American Geophysical Union. All rights reserved.

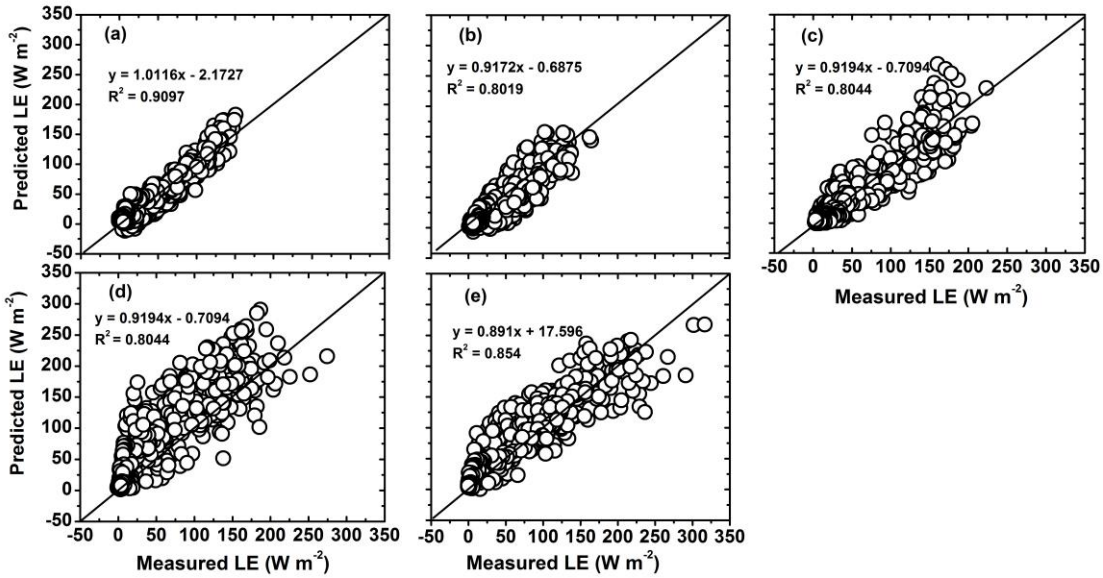

Figure 4. Comparisons between predicted and measured latent flux *(*LE) for (a) alpine meadow, (b) alpine swamp meadow, (c) cropland, (d) *T. ramosissima*, and (e) *P. euphratica* ecosystems at daily time scale for 2014 and 2015.

Accepted

© 2019 American Geophysical Union. All rights reserved.

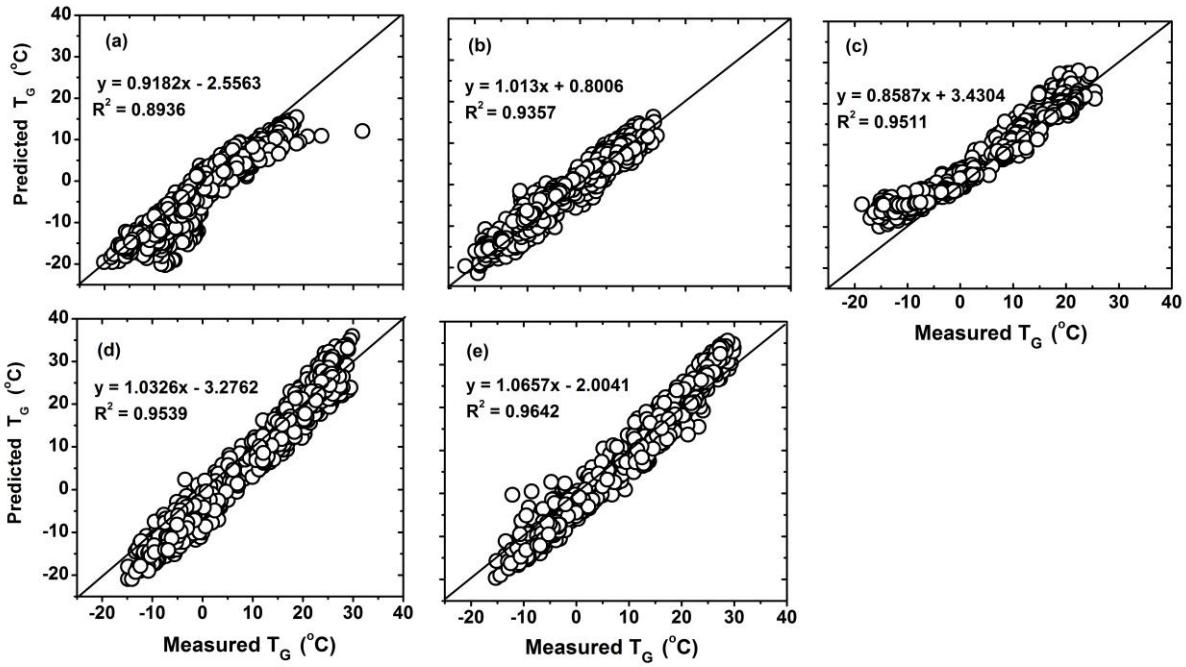

Figure 5. Comparisons between predicted and measured ground surface temperature (°C) for (a) alpine meadow, (b) alpine swamp meadow, (c) cropland, (d) *T. ramosissima*, and (e) *P. euphratica* ecosystems at daily time scale for 2014 and 2015.

Accepted

© 2019 American Geophysical Union. All rights reserved.

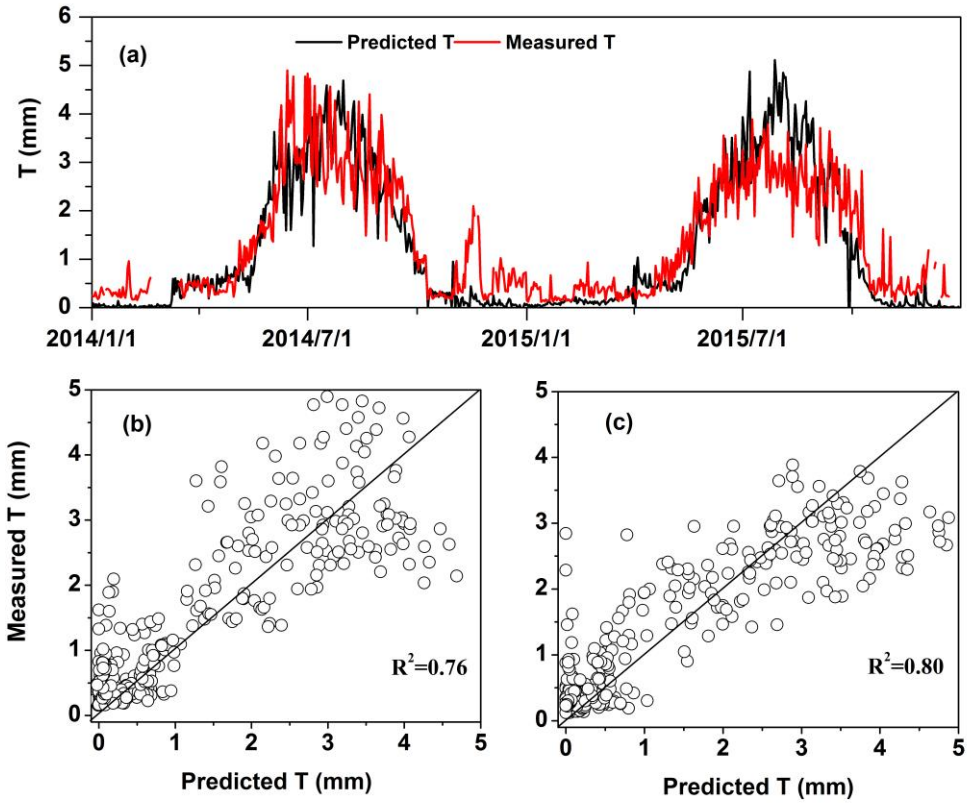

Figure 6. Comparison of transpiration (T) between measured by sap flow and by modeled for (a) day to day seasonal variations and 1:1 plot for dataset in (b) 2014 and (c) in 2015 at *P. euphratica* ecosystem.

Accepted

© 2019 American Geophysical Union. All rights reserved.

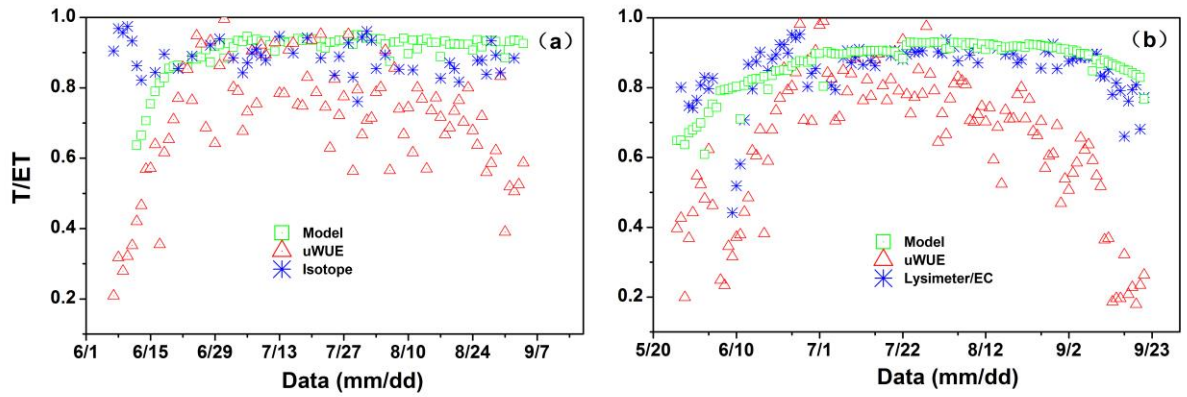

Figure 7. Comparison of T/ET values using the two source model and measured using underlying water use efficiency (uWUE) and isotope methods in the early afternoon (13:00–15:00) (a), and comparison of T/ET values using the two source model and measured using the uWUE and lysimeter/eddy covariance (EC) methods at daily scale (b) for the cropland ecosystem in 2012. The T/ET data using isotpe and lysimeter/eddy covariance (EC) methods were obtained from Wen et al., (2016). The estimated T/ET by uWUE approach was provided by Zhou et al. (2018).

Accepted

© 2019 American Geophysical Union. All rights reserved.

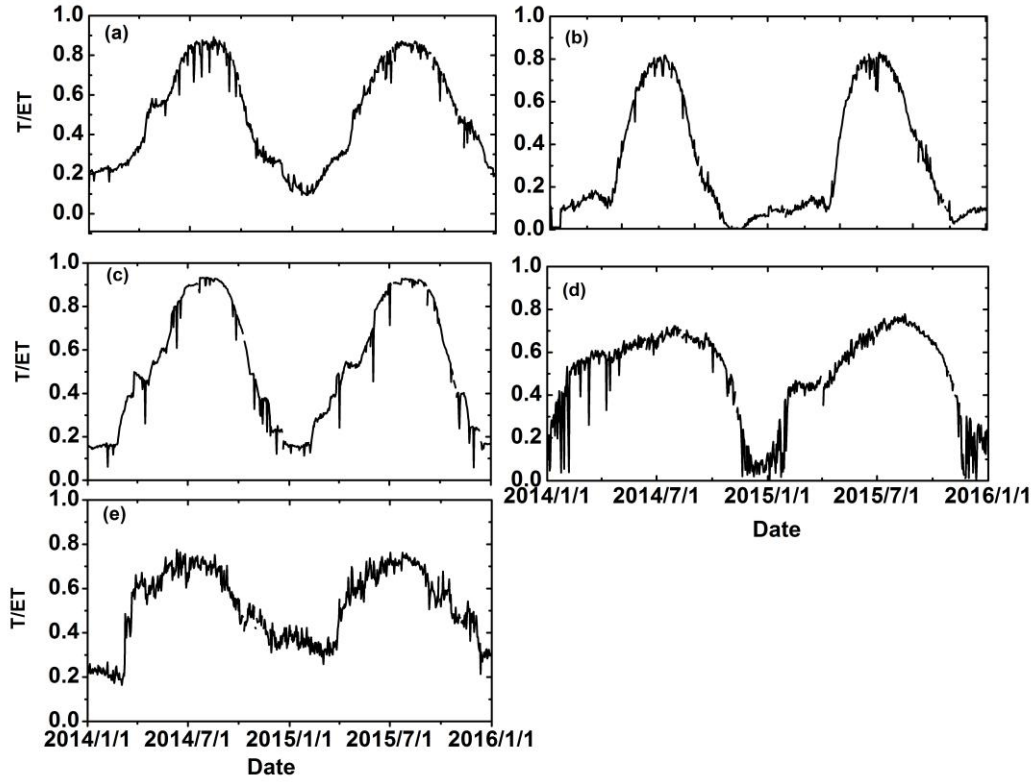

Figure 8. Daily variation of T/ET in typical ecosystems for (a) alpine meadow, (b) alpine swamp meadow, (c) cropland, (d) *T. ramosissima*, and (e) *P. euphratica* ecosystems from 2014 to 2015.

Accepted

© 2019 American Geophysical Union. All rights reserved.

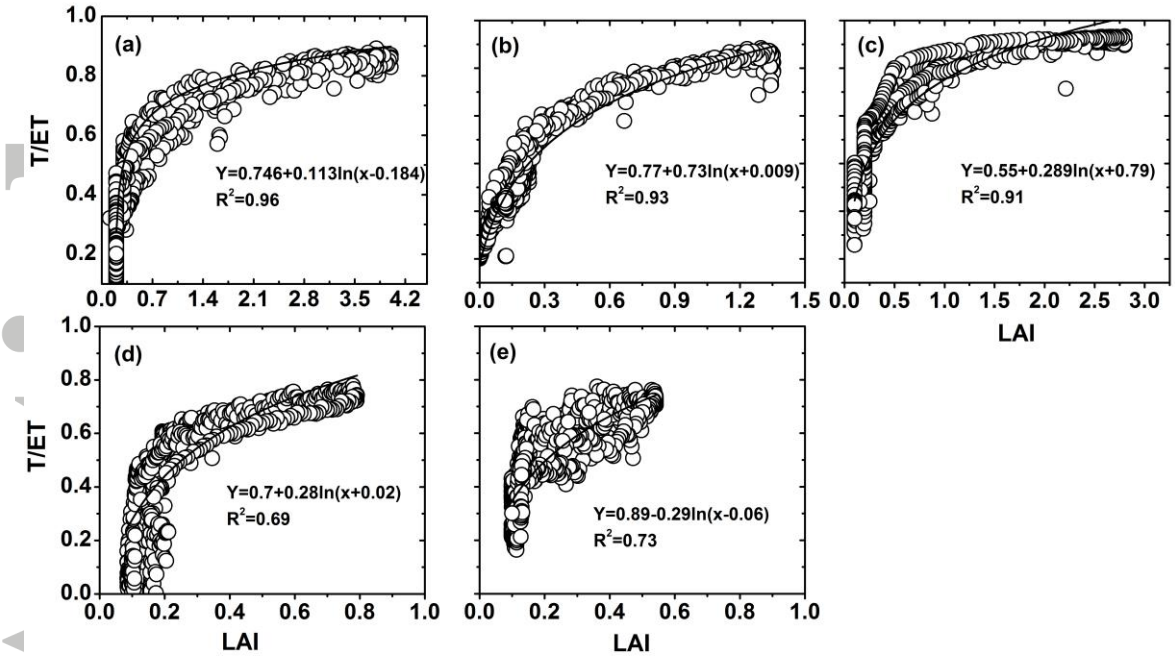

Figure 9. Relationship of LAI and T/ET at daily time scale for (a) alpine meadow ecosystem, (b) alpine swamp meadow, (c) cropland, (d) *T.ramosissima*, and (e) *P.euphratica* ecosystems from 2014 to 2015.

Accepted

© 2019 American Geophysical Union. All rights reserved.

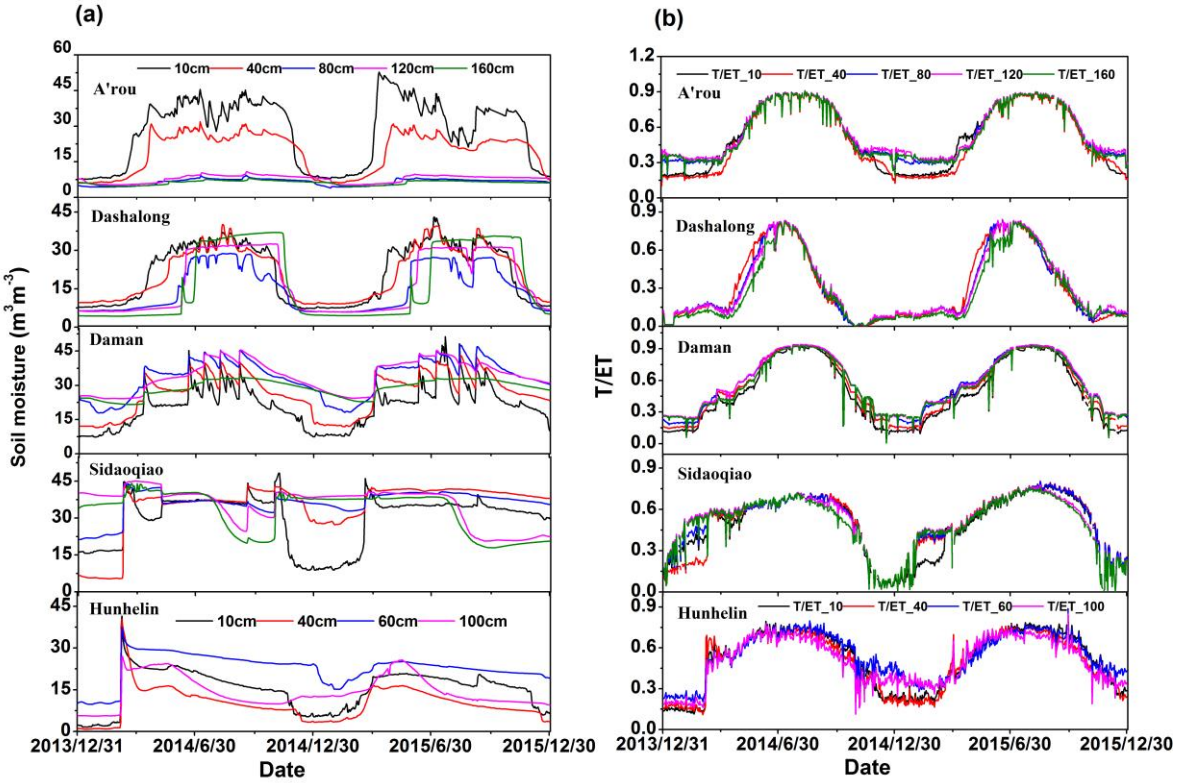

Figure 10. The soil moisture in different depth (a) and its corresponding transpiration fraction (T/ET)simulated by two source model (b) for alpine meadow ecosystem(A'rou), alpine swamp meadow (Dashalong), cropland (Daman), *T .ramosissima* and *P. euphratica* (Hunhelin) ecosystems from 2014 to 2015.

Accepted

© 2019 American Geophysical Union. All rights reserved.